Journal of Photochemistry and Photobiology A: Chemistry 220 (2011) 164–172

Contents lists available at ScienceDirect

Journal of Photochemistry and Photobiology A: Chemistry

journal homepage: www.elsevier.com/locate/jphotochem

Photochemical processes for dithiocarbamate metal complexes. Photochemistry of $Ni^{II}(n\text{-}Bu_2NCS_2)_2$ complex in CCl_4

Alexandr V. Kolomeets[a], Victor F. Plyusnin[a,b,*], Vjacheslav P. Grivin[a], Stanislav V. Larionov[c], Helge Lemmetyinen[d]

[a] Institute of Chemical Kinetics and Combustion SB RAS, 630090 Novosibirsk, Russian Federation
[b] Novosibirsk State University, 630090 Novosibirsk, Russian Federation
[c] Institute of Inorganic Chemistry SB RAS, 630090 Novosibirsk, Russian Federation
[d] Institute of Materials Chemistry, Tampere University of Technology, Finland

ARTICLE INFO

Article history:
Received 24 January 2011
Received in revised form 25 March 2011
Accepted 2 April 2011
Available online 13 April 2011

Keywords:
Photochemistry of dithiolathe complexes
Dithiocarbamate Ni(II) complex
Chlorine-containing solvent
Laser flash photolysis
Intermediates
Kinetics
Photolysis mechanism

ABSTRACT

Laser flash photolysis was used to study the nature and reactions of intermediates in photochemistry of the dithiocarbamate $Ni^{II}(S_2CN(n\text{-}Bu)_2)_2$ complex in CCl_4 (ligand $(n\text{-}Bu)_2NCS_2^- \equiv dtc^-$). It is shown that a nanosecond laser pulse (308 nm) results in absorption bands with maxima at 370 and 500 nm, belonging to the radical $ClNi^{II}(dtc)(dtc^\bullet)$ complex whose coordination sphere contains a dithiocarbamate radical $dtc^\bullet$, coordinated by one sulfur atom with the central metal ion. This intermediate complex forms, in the reaction with the initial $Ni(dtc)_2$ complex, the $ClNi^{II}(dtc)(dtc^\bullet)[Ni^{II}(dtc)_2]$ dimer during 20–30 μs. For several milliseconds the dimer adds another initial complex and transforms into the $Cl(dtc^\bullet)Ni^{II}(dtc)[Ni^{II}(dtc)_2]_2$ trimer. The reaction between two trimer molecules leads (for several tens of seconds) both to the recombination of coordinated $dtc^\bullet$ radicals and to the liberation of the final product, the thiuram disulfide molecule ($(n\text{-}Bu)_2NCS_2S_2CN(n\text{-}Bu)_2 \equiv tds$). The disproportionation of two $ClNi^{II}(dtc)$ complexes results in the precipitating $NiCl_2$ complex which is insoluble in CCl_4.

© 2011 Elsevier B.V. All rights reserved.

1. Introduction

Dithiocarbamate complexes of various metal ions are used in analytical chemistry [1,2], organic synthesis [3], medicine [4], biology [5], as antioxidants [6], polymer photostabilizers [7], and precursors for creating sulfide film semiconductors [8,9]. The complete current review on the transition metal dithiocarbamate chemistry is published in [10]. The capacity of these particles for self-assembly makes it possible to construct molecular containers for metal and fullerene ions [11–13]. Their optical and electrochemical properties favor the creation of cation, anion, and neutral molecule sensors [11,12,14,15]. Due to the high affinity of a dithiocarbamate ion for metal ions, these ligands can be used to stabilize silver and gold nanoparticles [16–18] as well as the conglomerates of gold nanoparticles with nucleic acids [19,20]. The high affinity of these ligands for metal surfaces can be used to stabilize quantum dots in the microscopy of biological objects [21,22]. The dithiocarbamate ligands form complexes with all transition metals and stabilize metal ions to the high oxidation levels. Well-known are the following dithiocarbamate complexes Ru(IV) [23], Au(III) [24,25], Cu(III) [26], Ni(IV) [26–28], and Fe(IV) [29]. In [30,31] the dithiocarbamate Ni(IV) complex is shown to possess photochromic properties.

Despite a great number of papers devoted to the chemistry and spectroscopy of dithiocarbamate complexes of transition metals, the photochemistry of these particles is as yet little understood [32–35]. In the literature, there are the papers which mainly report the results of stationary photolysis methods. Known are the works of the Bulgarian group (B. Zheliazkova) on the study of the photochemistry of the dithiocarbamate Cu(II) complexes by optical spectroscopy and EPR [36,37]. In these works, the mechanism of the photochemical transformations of the $Cu(dtc)_2$ complex in chlorine-containing solvents, involving removal of a dithiocarbamate radical from coordination sphere to solvent volume, is based on the results from stationary measurements. However, the $dtc^\bullet$ radical was not recorded in pulsed experiments and the mechanism of photolysis remains uncertain. Thus, for many dithiocarbamate complexes of transition metals, the pulsed methods should be employed both to elucidate the mechanism of photochemical reactions and to determine the nature of intermediates.

The goal of the present work is both to study the mechanism of photochemical transformations of the $Ni(n\text{-}Bu_2dtc)_2$ complex in CCl_4 and to determine the spectra, kinetics, and rate constants

* Corresponding author at: Institute of Chemical Kinetics and Combustion SB RAS, 630090 Novosibirsk, Russian Federation. Tel.: +7 383 3332385; fax: +7 383 3307350.
E-mail address: plyusnin@kinetics.nsc.ru (V.F. Plyusnin).

1010-6030/$ – see front matter © 2011 Elsevier B.V. All rights reserved.
doi:10.1016/j.jphotochem.2011.04.007

of reactions of excited states and intermediates using femto- and nanosecond laser flash photolysis.

2. Experimental

Nanosecond laser flash photolysis of solutions was performed on a setup with an excimer XeCl (308 nm, 15 ns, pulse energy – 50 mJ) or a neodymium YAG:Nd^{3+} (third harmonic 355 nm, 7 ns, 10 mJ) lasers [38]. The exciting and probing light beams entered solution in the cuvettes 1–10 mm thick at a minor angle (∼2°). Some experiments were carried out using a similar setup for laser flash photolysis [39] with the exciting and probing light beams of perpendicular geometry. After a photomultiplier, the signal was detected by a digital Tektronix 7912AD oscillograph connected to computer.

In laser flash photolysis, the spectra of intermediate absorption were recorded over millisecond and second ranges using an Ocean Optics USB4000 spectrophotometer. The exciting (355 nm) and probing light beams fell on a quartz microcuvette 1–10 mm thick and with a volume of 10–100 mm^3 at an angle of ∼8° to illuminate more than 90% of a solution.

A femtosecond laser photolysis (pump-probe spectroscopy) setup, described in [40], was used to study the ultra-fast relaxation processes of the excited states of the Ni(n-Bu_2dtc)$_2$ complex. The samples were excited by 100 fs pulses at a wavelength of 405 nm (the second harmonic of a Ti:Sapphire generator with an amplifier, CDP Ltd., Moscow, Russia) with a pulse repetition frequency of 10 Hz. One spectrum was recorded using about 200 repeating pulses. A solution was put in a rotating cuvette 1 mm thick to reach more homogeneous radiation and to exclude sample heating. The time-resolved spectra were first recorded with a shift of 100 fs during 3 ps and then with logarithmically increasing delays. Usually, about 60–70 spectra were recorded over the range of 20–40 ps. The program of experimental data processing introduced corrections for a group velocity dispersion and an instrument response function. The total time resolution ranged from 150 to 200 fs. All femtosecond experiments were carried out at room temperature.

The stationary irradiation of solutions was performed either with the pulses of a neodymium laser (355 nm, the third harmonic), an excimer XeCl laser (308 nm), a nitrogen laser (337 nm), a high-pressure mercury lamp (DRSh-500, lines 290, 313, 365 nm) or using a set of light emitting diodes of monochromatic radiation at 275, 306, 375, and 400 nm. Depending on the LED type and experimental conditions, the radiation power varied from 7 μW (for 275 nm) to 1 mW (400 nm). The optical absorption spectra were recorded using an HP 8453 spectrophotometer ("Agilent: Hewlett Packard") in quartz cuvettes with a 0.01–1 cm optical path.

When determining the quantum yield, the laser pulse energy was measured using a ferrioxalate actinometer and a Gentec-EO system (Canada) (a SOLO-2 monitor and a pyroelectric measuring QE25SP-H-MB head). Intensities of the mercury lamp light and the light emitting diode radiation were measured with the same system using a measuring photodiode PH100-SiUV head.

Composition of the mixture of components in irradiated solutions was analyzed by thin-layer chromatography using the "Silufol 60 F254" plates. Solutions were applied over the plates by means of a capillary (d = 1 mm). An aluminum plate was divided into several parallel paths, the first of which was covered with irradiated solution and the rest with individual solutions of the compounds contained, probably, in the mixture studied. A CCl_4–CH_2Cl_2 mixture (1:3) was used as an eluent. The Ni(n-Bu_2dtc)$_2$ complex was synthesized, purified, and analyzed by conventional techniques [41]. Solutions were prepared using spectrally pure solvents.

In numerical calculations of the kinetics of intermediate optical absorption disappearance, the differential equations were solved using a special program based on the forth-order Runge–Kutta method. The program allows calculations and the fitting to experimental kinetic curves at many wavelengths simultaneously. The time characteristics of the short-lived excited primary states were determined from intermediate absorption spectra by the program of the global treatment of kinetic curves array.

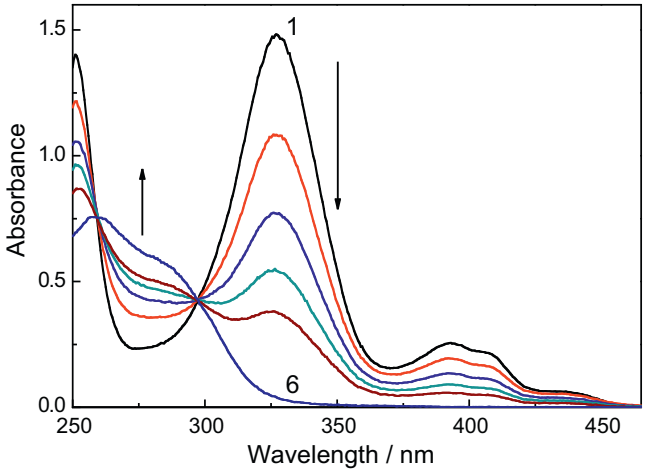

Fig. 1. The change in the optical spectrum of the Ni(n-Bu_2dtc)$_2$ (4×10^{-5} M) complex in CCl_4 upon stationary photolysis in a 1 cm cuvette. 1–5 – 0, 10, 20, 30, 40, 200 pulses of an XeCl excimer laser (308 nm), 6 – thiuram disulfide spectrum (4×10^{-5} M).

3. Results and discussion

3.1. Stationary photolysis of Ni(n-Bu_2dtc)$_2$ solutions

A flat Ni(n-Bu_2dtc)$_2$ complex is characterized by lengths of the Ni–S, S–C, and C–N bonds of 2.21, 1.73, and 1.33 Å and by a S–Ni–S angle of about 79° (sulfur atoms belong to the same ligand) [42]. Beyond the plane, there are only the butyl group atoms. The optical spectrum of this complex in CCl_4 contains absorption bands with maxima at 226, 250, 327, and 390 nm, with extinction coefficients of 28,400, 30,700, 37,200, and 6200 M^{-1} cm^{-1}, respectively. Absorption bands at 390 and 327 nm are the bands of charge transfer from ligand to metal (CTLM). Intraligand transitions can contribute to the bands at 226 and 250 nm [43]. The weak bands in the range of 435 and 476 nm refer to the d–d transitions [44].

The Ni(dtc)$_2$ complex exhibits no photochemical activity in acetonitrile, alcohol, and toluene solutions and starts to vanish under irradiation only in the presence of chlorine-containing solvents whose molecules are good electron acceptors. Fig. 1 shows a change in optical spectrum upon stationary photolysis of Ni(dtc)$_2$ in CCl_4. Irradiating solution by excimer laser pulses (308 nm) leads to the disappearance of the primary spectrum of the complex and the formation of broad absorption bands with maxima at 260 and 280 nm with isosbestic points preserved at 259 and 297 nm. The resulting novel absorption spectrum belongs to tetra-n-butylthiuramdisulfide (n-Bu_4tds = tds) (Fig. 1, spectrum 6) [45]. The similar changes in the optical spectrum are observed under irradiation with a less powerful UV-radiation of either light emitting diodes or mercury lamps. Since the radiation power for these light sources is by ∼8 orders of magnitude lower, the same spectral changes indicate the absence of two-quantum processes under laser excitation.

At high Ni(dtc)$_2$ concentrations (>10^{-4} M), photolysis leads to the formation of a grey–green precipitate of the $NiCl_2$ complex, which is actually insoluble in CCl_4. The thin-layer chromatography (TLC) of the irradiated and non-irradiated Ni(dtc)$_2$ and thiuram disulfide solutions was performed to identify the final products

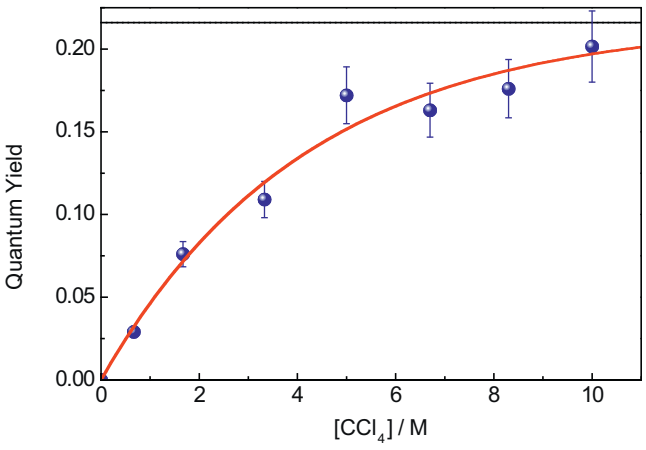

Fig. 2. The dependence of the quantum yield of $Ni(nBu_2dtc)_2$ photolysis on CCl_4 concentration in acetonitrile at irradiation wavelength of 306 nm. The solid line – approximation of a given dependence by a modified Perrin formula with radius $R = 5.5$ Å (see the text).

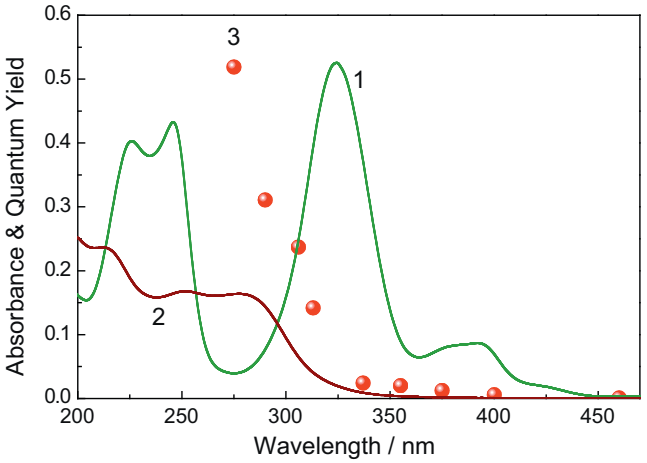

Fig. 3. The dependence of quantum yield (1) of the $Ni(n\text{-}Bu_2dtc)_2$ photolysis in CCl_4 on irradiation wavelength. Curves 2 and 3 – the spectra of the $Ni(n\text{-}Bu_2dtc)_2$ complex and the free $n\text{-}Bu_2dtc^-$ ligand in acetonitrile.

of photolysis. It verified the formation of the tds molecules and insoluble $NiCl_2$ precipitate.

The absence of photochemical activity of the $Ni(dtc)_2$ complex in acetonitrile allows us to define the behavior of quantum yield with increasing CCl_4 concentration (Fig. 2). At low CCl_4 concentrations in acetonitrile, the quantum yield increases linearly with passage to saturation at ~10 M. As shown below, the lifetime of the excited states of the complex is about 10 ps. During this period, a CCl_4 molecule diffuses to the excited complex over a distance no more than 2.5 Å. Thus, the electron acceptor (a CCl_4 molecule) must be located in the first coordination sphere along the axial axes of the flat complex. Under these conditions, the Perrin "black sphere" model can be used to process data on quantum yield. This model is applied for determining the energy transfer distance upon luminescence quenching in polymeric films and frozen matrices in which no diffusion is observed. For our case, we use a modified Perrin formula:

$$\varphi(C) = \varphi_\infty(1 - e^{-\Omega C}),$$

where C is the CCl_4 concentration, φ_∞ is the quantum yield at infinitely high acceptor concentration, $\Omega = 4/3(\pi R^3 N_0)$ is the volume of the black sphere within which an electron is transferred, R is the radius of the black sphere, and N_0 is the Avogadro number. The solid lines in Fig. 2 denote calculations from the modified Perrin formula with $R = 5.5$ Å.

Thus, the photochemistry of the $Ni(dtc)_2$ complex is determined by fast electron transfer from the excited complex to the nearest CCl_4 molecule located at a distance of about 5.5 Å. The CCl_4 radius is about 3.57 Å (the C–Cl bond length is 1.77 Å, and the chlorine atom radius is 1.8 Å [46]). In the radius of the black sphere, the share of the complex is about 2 Å, i.e., the CCl_4 molecule must be located just above the flat complex.

It is worth noting that a similar dependence of quantum yield on $CHCl_3$ concentration in acetonitrile was revealed by photolysis of the $[Ni(S_2C_2(CN)_2)_2]^{2-}$ complex [47]. The authors suggest that electron transfer from the excited complex to the $CHCl_3$ acceptor occurs in the collision complex and treat their results in terms

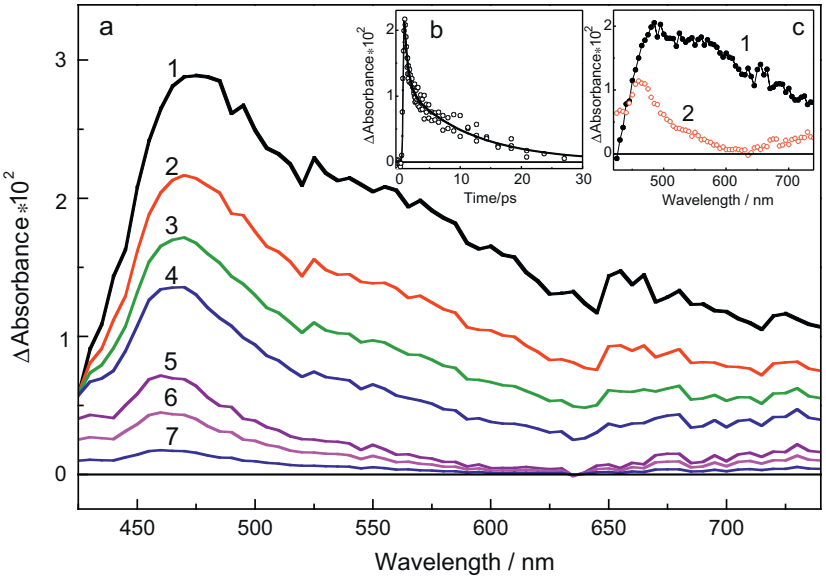

Fig. 4. The spectra of intermediate absorption (a) and experimental kinetics (dots) at 460 nm (b), recorded by femtosecond flash photolysis (405 nm) of the $Ni(n\text{-}Bu_2dtc)_2$ (3.07×10^{-3} M) solution in CCl_4 in a 1 mm cuvette. Spectra 1–7 – 0, 0.3, 0.6, 1, 5, 10, 20, 40 ps after the laser pulse. The solid line (b) – approximation in the framework of a two-exponential model with times of 0.63 and 14.9 ps. (c) – the spectra of fast (1) and slow (2) exponents are obtained by global treatment of kinetic curves at all wavelengths in the framework of a two-exponential model.

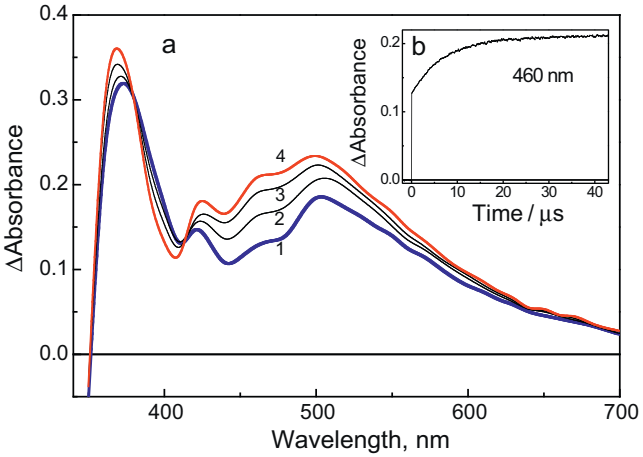

Fig. 5. The optical spectra of intermediate absorption (a) and the kinetics of absorption change at 460 nm (b), recorded by nanosecond laser flash photolysis (308 nm) Ni(n-Bu_2dtc)$_2$ (1.0×10^{-4} M) in CCl_4 in a 1 cm cuvette. (a) Spectra 1–4 – 0, 3, 11, 43 μs after the laser pulse.

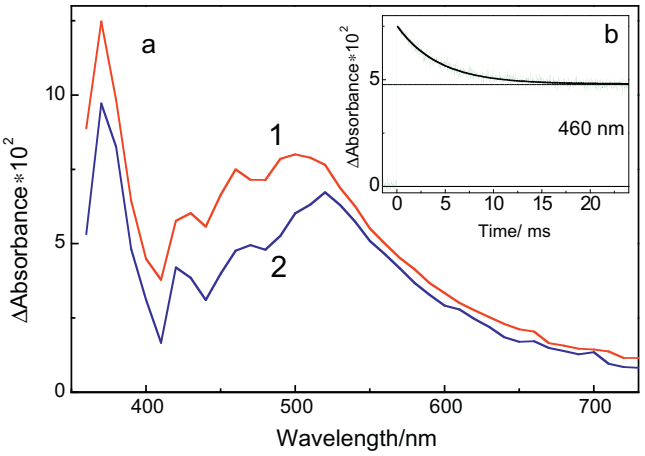

Fig. 7. The optical spectra of intermediate absorption (a) and the kinetics of absorption change at 460 nm (b), recorded by laser flash photolysis (355 nm) Ni(n-Bu_2dtc)$_2$ (5.0×10^{-5} M) in CCl_4 in a 1 cm cuvette in the millisecond time domain. (a) Spectra 1–2 – 50 μs and 25 ms after the laser pulse, respectively.

of the formula $\Phi/\Phi_{lim} = K_E C/(1 + K_E C)$, where K_E is an equilibrium constant of collision complex formation, and C is the $CHCl_3$ concentration. The quantum yield for $[Ni(S_2C_2(CN)_2)_2]^{2-}$ decreases 20 times with varying radiation wavelength from 313 to 365 nm. In this case, however, K_E remains unchanged. The quantum yield of the photolysis of the Ni(dtc)$_2$ complex in CCl_4 also increases substantially with decreasing wavelength of exciting light (Fig. 3). In the region of the d–d absorption bands (400–460 nm), it tends to zero and starts to increase at $\lambda > 320$ nm.

3.2. Ultra-fast relaxation processes of the excited Ni^{II}(n-Bu_2dtc)$_2$ complex

The Ni(dtc)$_2$ complex in acetonitrile exhibits no photochemical activity, probably, due to the fast relaxation processes. The time characteristics of these processes are determined by femtosecond laser photolysis. Exciting the Ni(dtc)$_2$ complex by the second harmonic of a Ti:Sapphire laser (100 fs, 405 nm) leads to the appearance of intermediate absorption which vanishes for several tens of picoseconds. For Ni(dtc)$_2$ in CCl_4, the spectral and kinetic characteristics are close to those obtained for acetonitrile. Fig. 4a shows the intermediate spectra recorded at various times after the pulse for Ni(dtc)$_2$ in CCl_4. The kinetic curve at 470 nm is presented in Fig. 4b. The laser pulse is followed by a broad absorption band over the range 425–800 nm with a maximum at about 475 nm, which fully vanishes during 30–40 ps. A global treatment of kinetic curves at all wavelengths gives satisfactory results in the framework of a two-exponential model with characteristic times of 0.63 ± 0.08 and 14.9 ± 3.3 ps. For acetonitrile solutions, these times are 0.75 ± 0.09 and 7.5 ± 1.6 ps. A broad band, belonging to the fast exponent (Fig. 4c, spectrum 1), corresponds to absorption from the excited complex state. It vanishes, probably, due to the vibrational relaxation in the excited state (the Frank–Condon state), the rearrangement of solvate environment, and the fast transition to the "hot" ground state. The spectrum of the second exponent substantially narrows (Fig. 4c, spectrum 2), and vanishes due to the vibrational cooling of the "hot" ground state.

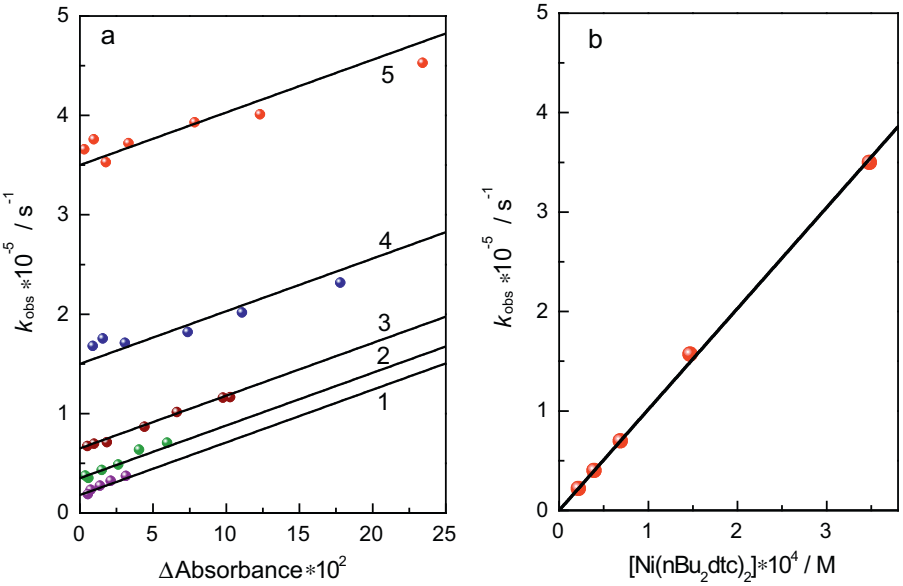

Fig. 6. The dependence of the observed constant k_{obs} on both the initial signal amplitude (a) and the Ni(n-Bu_2dtc)$_2$ concentration (b) at a wavelength of 460 nm. (a) 1–5 – correspond to complex concentrations of 2.16, 3.91, 6.87, 14.7, 34.8×10^{-5} M. (b) – the value of k_{obs} is determined by truncation on the ordinate in plot (a).

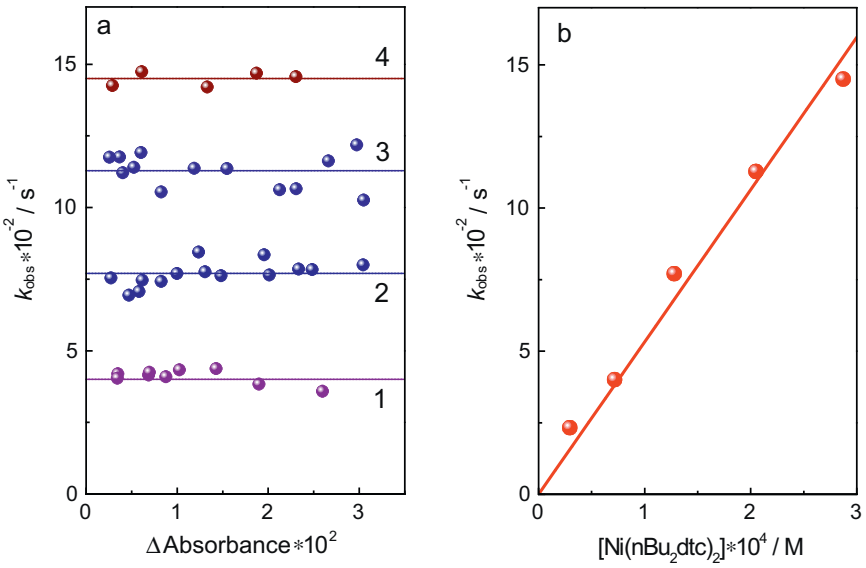

Fig. 8. The dependence of the observed rate constant k_{obs} on both the initial signal amplitude (a) and the Ni(nBu$_2$dtc)$_2$ concentration (b) upon laser flash photolysis (355 nm) at 460 nm within the millisecond time domain. The spectra and the kinetics are shown in Fig. 8. (a) 1–4 – correspond to concentrations of 7.18, 12.8, 20.5, 28.7 × 10^{-5} M. (b) The values of k_{obs} are determined by truncation on the ordinate in plot (a).

It is worth noting that the quantum yield of the Ni(dtc)$_2$ disappearance under irradiation at 405 nm (femtosecond pulse wavelength) is small enough (Fig. 3). Therefore, upon excitation at this wavelength, the process of electron transfer from the excited complex to the CCl_4 molecule cannot compete with fast relaxation processes. The development of the primary photochemical processes will be considered below upon nanosecond photolysis involving irradiation of shorter wavelengths.

3.3. *Nanosecond laser flash photolysis of Ni(n-Bu$_2$dtc)$_2$ solutions*

For the Ni(dtc)$_2$ solution in CCl_4 a nanosecond laser pulse (308 nm) is followed by intermediate absorption. The kinetics of its change covers a large time range from ~10 ns (laser pulse duration) to 100 s. Absorption, arising just after the pulse, contains bands with maxima at 500 and 370 nm (Fig. 5a, spectrum 1). An additional structure in the range 400–500 nm and the bleaching (a decrease in optical density) at $\lambda < 350$ nm are determined by the vanishing absorption of the initial complex. An increase in intensity and a change in absorption band shape at 500 and 370 nm with isosbestic points preserved at 380 and 413 nm are recorded for about 20–30 μs (Fig. 5a). Thus, the primary particle is transformed for about 20 μs into the second intermediate (kinetics at 460 nm is shown in Fig. 5b).

The primary intermediate spectrum transformation is accelerated considerably by an increase in concentration of the initial Ni(dtc)$_2$ complex. Fig. 6a demonstrates a linear dependence of the observed constant (k_{obs}) on the initial optical density at 460 nm after the laser pulse (ΔA_0) at various concentrations C_0 of the Ni(dtc)$_2$ complex (the dependence of k_{obs} on C_0 at $\Delta A_0 \to 0$ is shown in Fig. 6b). Thus, the primary particle vanishes in both the pseudo-first order reaction (rate constant k_1), interacting with the initial complex, and the second-order reaction (k_2). The observed rate constant for this case obeys the equation

$$k_{obs} = k_1 \times C_0 + 2k_2 \frac{\Delta A_0}{\varepsilon \times l},$$

where ε is the absorption coefficient of the initial intermediate at a recording wavelength, and l is the thickness of the cuvette. The slope of the straight line in Fig. 6b allows us to determine a bimolecular rate constant of the reaction between the primary intermediate and the initial complex, $k_1 = 1.05 \times 10^9$ M^{-1} s^{-1}, and the slopes of the straight lines in Fig. 6a can be used to determine $2k_2/\varepsilon = 5.3 \times 10^5$ cm × s^{-1}.

The secondary intermediate, formed during 20–30 μs, is the long-lived one and its absorption starts to vary only in the millisecond time domain. Fig. 7a shows both the spectrum, formed within 50 μs after the laser pulse (belonging to the secondary particle) and its change within 25 ms (kinetic curve is shown in Fig. 7b). Thus, within 25 ms after the laser pulse, the second intermediate transforms into the third intermediate whose spectrum conserves absorption bands with maxima at 370 and 500 nm.

To define the nature of the process from which the third particle arises, we have measured the dependence of the observed rate constant (k_{obs}) on the initial signal amplitude at 460 nm (the optical density ΔA_0 of the second intermediate at 50 μs) for various concentrations of the initial complex (Fig. 8a). The observed rate constant (k_{obs}) is independent of ΔA_0 and increases linearly with increasing concentration of the initial Ni(dtc)$_2$ complex (Fig. 8b). Thus, in the reaction with the initial complex, the second intermediate transforms into the third one. The slope of the straight line in Fig. 8b corresponds to the value of the bimolecular rate constant $k_3 = (5.3 \pm 0.2) \times 10^6$ M^{-1} s^{-1}.

The disappearance of the third intermediate is a concluding process of a given system. Fig. 9a demonstrates a change in intermediate absorption over the time range 25 ms to 200 s. Within about 100 s, the process is completed with the formation of final products. The kinetics of the change in optical density at 330 nm is shown in Fig. 9b. In this case, the reaction is determined by the second-order kinetic law which is verified by the linear dependence of the observed rate constant on the initial signal amplitude. Thus, the third intermediate vanishes in the second-order reaction with the observed rate constant

$$k_{obs} = 2k_4 \frac{\Delta A_0}{\varepsilon \times l},$$

where k_4 is the constant of a bimolecular reaction, and ε is the coefficient of the third intermediate extinction at the wavelength recorded. Treating the linear dependences of k_{obs} on ΔA_0 at various

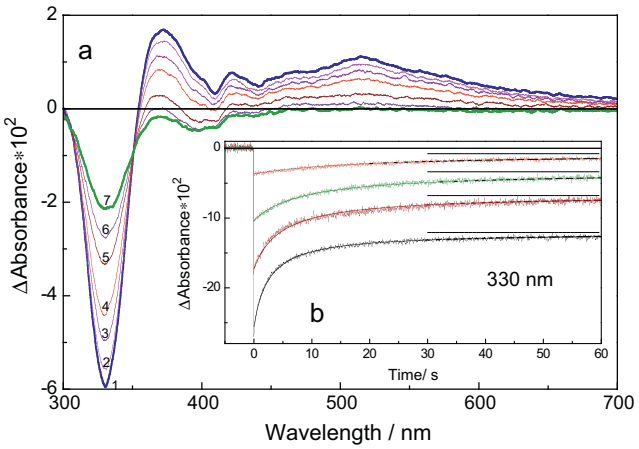

Fig. 9. The optical spectra of intermediate absorption (a) and the kinetics of absorption change at 330 nm (b), recorded upon laser flash photolysis (355 nm) of Ni(n-Bu_2dtc)$_2$ (9.5×10^{-5} M) in CCl_4 in a 1 cm microcuvette within a second time domain. (a) Spectra 1–7 – 1, 2, 5, 10, 30, 60, 200 s after the laser pulse. (b) The solid lines – calculations in the framework of the second-order kinetics.

wavelengths, we obtain

$$\frac{2k_4}{\varepsilon} = 1.1 \pm 0.2(330\,\text{nm}); \quad 3.4 \pm 0.3(370\,\text{nm});$$

$$7.4 \pm 0.5(520\,\text{nm})\,\text{cm} \times \text{s}^{-1}$$

The works on the photochemistry of the dithiocarbamate complexes of transition metals, performed by stationary methods, suggest that the primary process gives rise to a free dithiocarbamate radical dtc• [36,37]. In acetonitrile, this radical exhibits absorption band with a maximum at 590 nm [48]. The flash photolysis of the thiuram disulfide solution in CCl_4 indicates that a free dtc• radical also displays a band in this solvent and at the same 590 nm with an extinction coefficient of 3100 M^{-1} cm^{-1}. Thus, the broad band with a maximum at 500 nm, typical of all three intermediates, belongs, probably, not to the free dtc• radical, but to that coordinated by a sulfur atom with a nickel ion.

3.4. The nature of processes occurring upon photolysis of the Ni(n-Bu_2dtc)$_2$ complex in CCl_4

The optical spectrum of the Ni(dtc)$_2$ complex is almost independent of solvent nature, and the quantum light absorption in the UV range (308 nm) corresponds to either the excitation in the state where a charge is transferred from ligand to nickel atom (CTLM) or the ligand excitation (LL*)

$$Ni^{II}(dtc)_2 \overset{h\nu}{\rightleftarrows} Ni^{I}(dtc)(dtc^{\bullet}) \quad (\text{CTLM}) \qquad (1)$$

$$Ni^{II}(dtc)_2 \overset{h\nu}{\rightleftarrows} Ni^{II}(dtc)(dtc^{*})(LL^{*}) \qquad (2)$$

Fig. 3 demonstrates the spectra of both the complex and the free ligands. The LL* excitation is observed to contribute to the complex at $\lambda < 350$ nm. The data on the quantum yield presented in this Fig. 3, indicate that it starts to increase substantially from this wavelength to the short-wave spectrum region. Since upon nanosecond measurements the quantum yield at 308 nm is less than unity, the excited CTLM state relaxes to the ground one with inverse charge transfer to the ligand during ~10–15 ps (Fig. 4). However, if the Ni–S bond is broken, a fast inverse electron transfer becomes impossible, and an intermediate particle arises (the radical Ni^{I}(dtc)(dtc•) complex) in which the dtc• radical is coordinated via one sulfur atom with the Ni(I) ion. Since a photochemical activity is manifested only

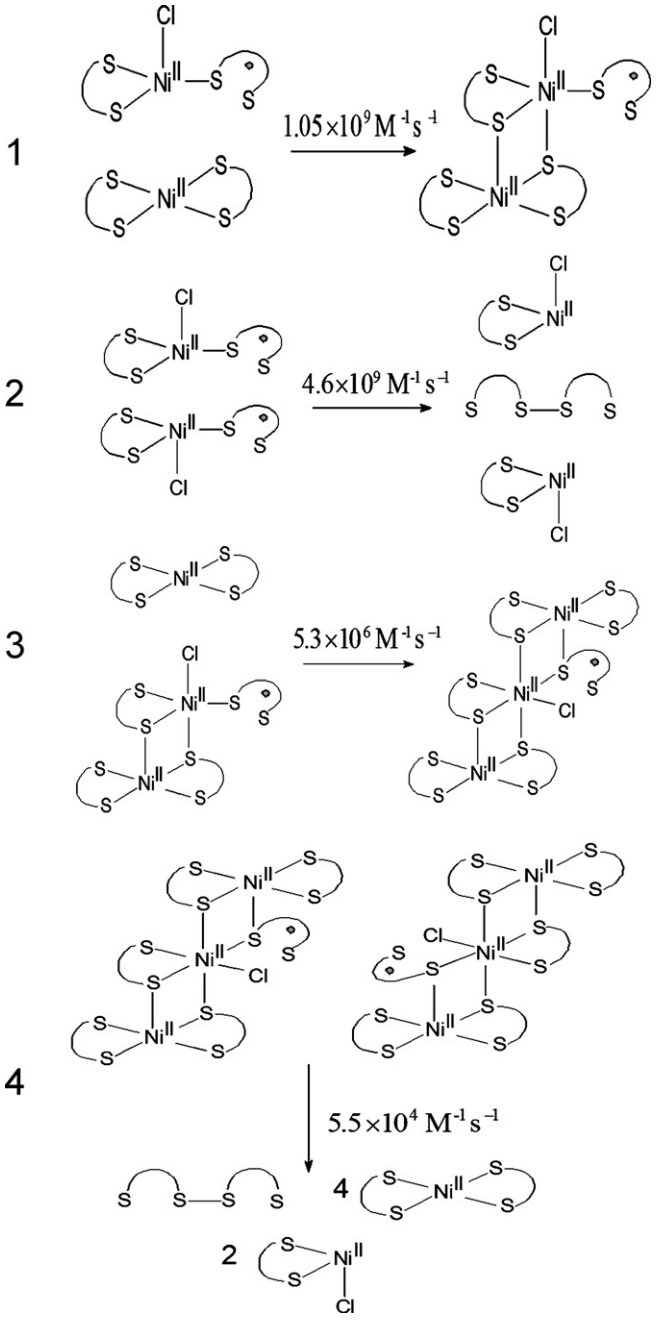

Fig. 10. A scheme of photochemical transformation of the Ni(n-Bu_2dtc)$_2$ complex in CCl_4. (1) Reaction between the radical complex and the initial complex resulting in the dimer, (2) recombination of the radical complexes resulting in the formation of thiuram disulfide, (3) reaction between the dimer and the initial complex giving rise to the trimer; (4) the final reaction of two trimer molecules resulting in the formation of final products.

in the presence of the CCl_4 molecules, that are the effective electron acceptors, the next transformation stage is the electron transfer and the formation of a successive intermediate

$$Ni^{I}(dtc)(dtc^{\bullet})\ldots CCl_4 \rightarrow [Ni^{II}(dtc)(dtc^{\bullet})]^{+}\ldots CCl_4^{\bullet -} \qquad (3)$$

Upon LL* excitation, the electron transfer to CCl_4 can occur just from the excited ligand

$$Ni^{II}(dtc)(dtc^{*})\ldots CCl_4 \rightarrow [Ni^{II}(dtc)(dtc^{\bullet})]^{+}\ldots CCl_4^{\bullet -} \qquad (4)$$

In both of the cases, the $[Ni^{II}(dtc)(dtc^{\bullet})]^{+}$ complex is formed and it is rather difficult to distinguish between these two cases. How-

Table 1
Absorption coefficients (M^{-1} cm^{-1}) of intermediates participating in photochemical transformations of the Ni(n-Bu_2dtc)$_2$ complex in CCl_4.

Intermediate	Wavelength/nm		
	370	460	520
Ni(n-Bu_2dtc)$_2$	3900	140	56
ClNi(dtc)(dtc•)	15700 ± 1500	8600 ± 500	6800 ± 700
Cl(dtc)(dtc•)Ni(dtc)Ni(dtc)$_2$ (dimer D)	21800 ± 2000	8300 ± 800	8000 ± 800
Cl(dtc)(dtc•)Ni(dtc)[Ni(dtc)$_2$]$_2$ (trimer T)	17000 ± 1500	5300 ± 500	7000 ± 700

ever, a substantial increase in quantum yield in the short-wave region, in which an increase in the LL* absorption contribution is expected, can testify to the predominance of process (4).

As follows from radiation chemistry [49], the $CCl_4^{\bullet-}$ anion radical dissociates rapidly into a Cl^- ion and a neutral $CCl_3^\bullet$ radical. The oppositely charged Cl^- ion and the $[Ni^{II}(dtc)(dtc^\bullet)]^+$ complex are in the cage of the nonpolar solvent and can form the third generation of the $[ClNi^{II}(dtc)(dtc^\bullet)]$ intermediates

$$CCl_4^{\bullet-} \rightarrow Cl^- + CCl_3^\bullet \quad (5)$$

$$[Ni^{II}(dtc)(dtc^\bullet)]^+ + Cl^- \rightarrow [ClNi^{II}(dtc)(dtc^\bullet)] \quad (6)$$

The chloride ion of the $[ClNi^{II}(dtc)(dtc^\bullet)]$ complex is at the axial position (so as a parent CCl_4 molecule). Reactions (3)–(6) are the fast processes and are likely to proceed within the subpico- and picosecond time domains.

Thus, by the time of registration with a nanosecond time resolution, a solution contains the $[ClNi^{II}(dtc)(dtc^\bullet)]$ complex. In this case, the absorption band with a maximum at 500 nm (Fig. 5) belongs, most probably, to the dtc• radical, coordinated via one sulfur atom with the nickel ion (for a free radical, the absorption band has a maximum at 590 nm). The fast processes of $ClNi^{II}(dtc)(dtc^\bullet)$ formation cannot be recorded due to the low quantum yield (~0.006) at 405 nm upon femtosecond flash photolysis.

Upon registration with nanosecond time resolution, the primary $ClNi^{II}(dtc)(dtc^\bullet)$ complex vanishes in the pseudo-first order reaction as the observed rate constant increases with increasing Ni(dtc)$_2$ concentration. For k_{obs}, the linear dependence of truncation on the ordinate on the concentration of the initial Ni(dtc)$_2$ complex (Fig. 6a) corresponds to the bimolecular rate constant $k_1 = (1.05 \pm 0.05) \times 10^9$ M^{-1} s^{-1} (less by order of magnitude than the diffusion limit). The various mechanisms can be suggested for the reaction between $[ClNi^{II}(dtc)(dtc^\bullet)]$ and the initial complex. The reaction of the dtc• radical transfer to the coordination Ni(dtc)$_2$ sphere can be neglected, because the flash photolysis of the Ni(dtc)$_2$–thiuram disulfide system in CCl_4 indicates that the dtc• radical vanishes (recombines) despite the presence of the Ni(dtc)$_2$ complex. The electron transfer from the ligand of the initial complex to the radical of the intermediate complex

$$[ClNi^{II}(dtc)(dtc^\bullet)] + Ni^{II}(dtc)_2 \rightarrow [ClNi^{II}(dtc)_2] + [Ni^{II}(dtc)(dtc^\bullet)] \quad (7)$$

is the degenerate reaction without actual change in the nature of the intermediate. More feasible is the process of dimer (D) formation

$$ClNi^{II}(dtc)(dtc^\bullet) + Ni^{II}(dtc)_2 \rightarrow Cl(dtc^\bullet)Ni^{II}(dtc)[Ni^{II}(dtc)_2] \quad \text{(dimer D)} \quad (8)$$

The band at 500 nm belongs to the coordinated dtc• radical. Therefore, its position changes but little during reaction (8), because the radical remains in the coordinated state. The slope of the linear dependence of k_{obs} on signal amplitude (Fig. 6a) is determined by the second-order reaction between two $ClNi^{II}(dtc)(dtc^\bullet)$ complexes. Since the photochemical transformations result in thiuram disulfide with an 1:1 yield with respect to the initial complex, this reaction is assumed to involve recombination of the coordinated dtc• radicals

$$ClNi^{II}(dtc)(dtc^\bullet) + ClNi^{II}(dtc)(dtc^\bullet) \rightarrow tds + 2ClNi^{II}(dtc) \quad (9)$$

Thus, the primary particle of the nanosecond flash photolysis, i.e., the radical $ClNi^{II}(dtc)(dtc^\bullet)$ complex, vanishes for 20–30 μs in two competing reactions (8) and (9) that form either dimer D or the final product, thiuram disulfide. When the concentrations of the initial Ni(dtc)$_2$ complex exceed 10^{-4} M and the laser pulse intensities are low (low $ClNi^{II}(dtc)(dtc^\bullet)$ concentrations), the formation of the dimer is predominant.

The formation of dimers is typical of the chemistry of dithiocarbamate and dithiolate complexes of bivalent nickel and other transition metals. Thus, e.g., the formation of the dimers (dtc)Ni($S_2C_2(CF_3)_2$)$_2$Ni(dtc) and (xan)Ni($S_2C_2(CF_3)_2$)$_2$Ni(xan) is shown in [50], where xan is the xanthogene ligand–S_2COEt. The reaction between Ni(acac)$_2$ and pyridine-2,6-dimethanethiol (H_2pdmt) in toluene results in the [Ni(pdmt)]$_2$ dimer [51]. The following dimer complexes were synthesized, {[(diphosphine)Ni]$_2$(dithiolate)}(X)$_2$ (X = BF_4 or PF_6) [52], [Ni(pdmt)]$_2$ and [Ni(pdtc)]$_2$ (pdmt = pyridine-2,6-dimethanethiolate and pdtc = pyridine-2,6-dithiocarboxylate) [53]. The formation of either metal–metal or metal–sulfur bonded dimers depends on the balance of many factors. Much is determined by electron repulsion on the nonbinding orbitals of sulfur atoms, the size and population of ion d-orbitals, and the steric repulsion of substituents in either dithiolene or dithiolate ligands [54]. It is worth noting that the formation of dimers is typical of not only the dithiocarbamate complexes of bivalent nickel but also of the complexes with these ligands and other metals, e.g., Ru(III) [33] and Cu(II) [55]. Thus, the assumption of dimer formation does not violate the boundaries of the well-known chemistry of dithiocarbamate and dithiolate complexes of transition metals.

Table 2
Rate constants of the formation and disappearance of intermediates upon flash photolysis of the Ni(nBu_2dtc)$_2$ complex in CCl_4.

Reaction	Rate constant (M^{-1} s^{-1})
ClNi(dtc)(dtc•) + Ni(dtc)$_2$ → Cl(dtc)(dtc•)Ni(dtc)Ni(dtc)$_2$ (D)	$k_1 = (1.05 \pm 0.05) \times 10^9$
ClNi(dtc)(dtc•) + ClNi(dtc)(dtc•) → tds + 2 ClNi(dtc)	$2k_2 = (4.6 \pm 0.2) \times 10^9$
D + Ni(dtc)$_2$ → Cl(dtc)(dtc•)Ni(dtc)[Ni(dtc)$_2$]$_2$ (T)	$k_3 = (5.3 \pm 0.2) \times 10^6$
T + T → tds + 2ClNi(dtc) + 4Ni(dtc)$_2$	$2k_4 = (5.5 \pm 0.5) \times 10^4$

The absorption of dimer D starts to vary within the millisecond time domain (Fig. 7). In this case, the observed rate constant is also dependent on the concentration of the initial complex (Fig. 8), which is indicative of trimer formation

$$D + Ni^{II}(dtc)_2 \rightarrow Cl(dtc^{\bullet})Ni^{II}(dtc)[Ni^{II}(dtc)_2]_2 \quad \text{(trimer T)} \qquad (10)$$

Note that the formation of both trimers [53,56] and the complexes with a great number of nickel ions [56] is well known from the chemistry of the complexes of bivalent nickel with sulfur-containing ligands.

For trimer T, the absorption band at 500 nm is conserved (Fig. 7), because the dtc• radical remains coordinated with the bivalent nickel ion. The trimer is the third (last) intermediate which vanishes during several tens of seconds in the second-order reaction. Fig. 9 shows the disappearing of the trimer spectrum and kinetics over the range up to 200 s. The solid lines in the kinetic curves (Fig. 9b) were calculated in the framework of the second-order reaction and are in fair agreement with the experimental ones. Since the final product is represented by a thiuram disulfide molecule, it is assumed that the dithiocarbamate radicals of two trimers recombine via free sulfur atoms to form the tds molecules. As there is no new absorption, the Ni–S bonds of coordinated thiuram disulfide dissociate to form final products

$$T + T \rightarrow tds + 2ClNi^{II}(dtc) + 4Ni^{II}(dtc)_2 \qquad (11)$$

As mentioned above, at relatively high initial concentrations of the initial $Ni(dtc)_2$ complex, the photolysis gives rise to the $NiCl_2$ precipitate

$$2ClNi^{II}(dtc) \rightarrow Ni^{II}(dtc)_2 + Ni^{II}Cl_2 \downarrow \qquad (12)$$

The proposed scheme of a successive formation of the radical $ClNi^{II}(dtc)(dtc^{\bullet})$ complex, dimer D and trimer T can be used to calculate kinetic curves within various time domains and to compare them with the experimental kinetics. A global fitting with the same rate constants at all wavelengths allowed us to determine the extinction coefficients and the spectra of intermediates. Table 1 summarizes the values of extinction coefficients for the $Ni(dtc)_2$ complex and all intermediates. Calculating the extinction coefficients of the radical complex and trimer absorption, we determine the rate constants of the second-order reaction in which these particles vanish. Table 2 presents the reaction rate constants that determine the transformations of intermediates and are used to calculate kinetic curves. Fig. 10 plots a succession of the transformations of intermediates upon photochemical transformation of the $Ni(dtc)_2$ complex in CCl_4.

4. Conclusions

The nature, the spectral and kinetic parameters of intermediates, resulting from quantum light absorption by the $Ni(n\text{-}Bu_2dtc)_2$ complex in CCl_4 solution have been studied using the femto-and nanosecond flash photolysis within the ultra-wide time domain (100 fs to 100 s). The femtosecond excitation at 405 nm is shown to cause fast relaxation to the ground state during about 15 ps. With the use of a nanosecond pulse at 308 nm, an electron is transferred from the excited complex to the CCl_4 molecule which gives the first intermediate (the radical $ClNi^{II}(dtc)(dtc^{\bullet})$ complex) where the dithiocarbamate radical is coordinated by one sulfur atom with the Ni(II) ion. The quantum yield starts to increase substantially at wavelength shorter than 350 nm. The radical complex in the reaction with the initial complex forms first the $Cl(dtc^{\bullet})Ni^{II}(dtc)[Ni^{II}(dtc)_2]$ dimer and then the $Cl(dtc^{\bullet})Ni^{II}(dtc)[Ni^{II}(dtc)_2]_2$ trimer. The recombination of two trimer molecules leads to the formation of the final products: the molecules of thiuram disulfide and the $ClNi^{II}(dtc)$ complex. Thus, the mechanism of the photochemical transformation of the $Ni(n\text{-}Bu_2dtc)_2$ complex appeared to be much more tedious than is shown in the works on the stationary photolysis of dithiocarbamate complexes of transition metals.

Acknowledgments

The work was supported by the Russian Foundation for Fundamental Research (grants 11-03-00268, 09-03-00330, and 07-02-91016-AΦ) and the program of International Integration Projects of SB RAS (grant 70).

References

[1] K.W. Weissmahr, C.L. Houghton, D.L. Sedlak, Analysis of the dithiocarbamate fungicides Ziram, Maneb, and Zineb and the flotation agent ethylxanthogenate by ion-pair reversed-phase HPLC, Anal. Chem. 70 (1998) 4800–4804.
[2] J.M. Lo, J.D. Lee, Dithiocarbamate extraction and Au(III) back extraction for determination of mercury in water and biological samples by anodic stripping voltammetry, Anal. Chem. 66 (1994) 1242–1248.
[3] A. Henckens, K. Colladet, S. Fourier, T.J. Cleij, L. Lutsen, J. Gelan, D. Vanderzande, Synthesis of 3,4-diphenyl-substituted poly(thienylene vinylene), low-band-gap polymers via the dithiocarbamate route, Macromolecules 38 (2005) 19–26.
[4] B. Cvek, V. Milacic, J. Taraba, Q.P. Dou, Ni(II), Cu(II), and Zn(II) diethyldithiocarbamate complexes show various activities against the proteasome in breast cancer cells, J. Med. Chem. 51 (2008) 6256–6258.
[5] G.D. Thorn, R.A. Ludwig, The Dithiocarbamates and Related Compounds, Elsevier, Amsterdam, 1962, 298 pp.
[6] J. Kateva, S.K. Ivanov, Mechanism of inhibitory action of metal dithiocarbamates. II. Autooxidation of tetralin and cumene and decomposition of tetralin hydroperoxide in presence of zinc bisisobutyldithiocarbamate, J. Polym. Sci.: Polym. Chem. Ed. 17 (1979) 2707–2718.
[7] F.X. O'Shea, Dialkylhydroxybenzyl-N,N-dimethyl dithiocarbamates as intermediates in the preparation of phenolic polymer stabilizers, Adv. Chem. 85 (1968) 126–139.
[8] G. Barone, T. Chaplin, T.G. Hibbert, A.T. Kana, M.F. Mahon, K.C. Molloy, I.D. Worsley, I.P. Parkin, L.S. Price, Synthesis and thermal decomposition studies of homo- and heteroleptic tin(IV) thiolates and dithiocarbamates: molecular precursors for tin sulfides, J. Chem. Soc., Dalton Trans. (2002) 1085–1092.
[9] M.D. Regulacio, N. Tomson, S.L. Stoll, Dithiocarbamate precursors for rare-earth sulfides, Chem. Mater. 17 (2005) 3114–3121.
[10] G. Hogarth, Transition metal dithiocarbamates: 1978–2003, Prog. Inorg. Chem. 53 (2005) 71–561.
[11] J. Cookson, P.D. Beer, Exploiting the dithiocarbamate ligand in metal-directed self-assembly, Dalton Trans. (2007) 1459–1472.
[12] O.D. Fox, M.G.B. Drew, E.J.S. Wilkinson, P.D. Beer, Cadmium- and zink-directed assembly of nano-sized, resorcarene-based host architectures which strongly bind C_{60}, Chem. Commun. (2000) 391–392.
[13] O.D. Fox, M.G.B. Drew, P.D. Beer, Resorcarene-based nanoarchitectures: metal-directed assembly of a molecular loop and tetrahedron, Angew. Chem. Int. Ed. 39 (2000) 136–140.
[14] W.W.H. Wong, D. Curiel, S.-W. Lai, M.G.B. Drew, P.D. Beer, Ditopic redox-active polyferrocenyl zink(II) dithiocarbamate macrocyclic receptors: synthesis, coordination and electrocemical recognition properties, Dalton Trans. (2005) 774–781.
[15] P.D. Beer, N. Berry, M.G.B. Drew, O.D. Fox, M.E. Padilla-Tosta, S. Patell, Self-assembled dithiocarbamate-copper(II) macrocycles for electrochemical anion recognition, Chem. Commun. (2001) 199–200.
[16] M.C. Tong, W. Chen, J. Sun, D. Ghosh, S. Chen, Dithiocarbamate-capped silver nanoparticles, J. Phys. Chem. B. 110 (2006) 19238–19242.
[17] L. Guerrini, J.V. Garicia-Ramos, C. Domingo, S. Sanchez-Cortes, Self-assembly of a dithiocarbamate calix[4]arene on Ag nanoparticles and its application in the fabrication of surface-enhanced Raman scattering based nanosensors, Phys. Chem. Chem. Phys. 11 (2009) 1787–1793.
[18] M.S. Vichers, J. Cookson, P.D. Beer, P.T. Bishop, B. Thiebaut, Dithiocarbamate ligand stabilised gold nanoparticles, J. Mater. Chem. 16 (2006) 209–215.
[19] J. Sharma, R. Chhabra, H. Yan, Y. Liu, A facile in situ generation of dithiocarbamate ligands for stable gold nanoparticle-oligonucleotide conjugates, Chem. Commun. (2008) 2140–2142.
[20] P. Morf, F. Raimondi, H.-G. Nothofer, B. Schnyder, A. Yasuda, J.M. Wessels, T.A. Jung, Dithiocarbamates: functional and versatile linkers for the formation of self-assembled monolayers, Langmuir 22 (2006) 658–663.
[21] F. Dubois, B. Mahler, B. Dubertret, E. Doris, C. Mioskowski, A versatile, strategy for quantum dot ligand exchange, J. Am. Chem. Soc. 129 (2007) 482–483.
[22] G. Han, T. Mokari, C. Ajo-Franklin, B.E. Cohen, Caged quantum dots, J. Am. Chem. Soc. 130 (2008) 15811–15813.
[23] K.W. Given, B.M. Mattson, L.H. Pignolet, Synthesis, properties, and X-ray structural characterization of a novel seven-coordinate halogenotris(dithiocarbamato) complex of ruthenium(IV), Inorg. Chem. 15 (1976) 3152–3156.
[24] P.T. Beurskens, J.A. Cras, J.G.M. van der Linden, Preparation, structure, and properties of bis(N,N-di-n-butyldithiocarbamato)gold(III) bromide

and bis(N,N-di-n-butyldithiocarbamato) gold(III) tetrabromoaurate(III), Inorg. Chem. 9 (1970) 475–479.
[25] M. Bardaji, A. Laguna, M. Laguna, F. Merchan, Methyl dithiocarbamate gold(I) and gold(III) complexes. Synthesis and reactivity with amines, Inorg. Chim. Acta 215 (1994) 215–218.
[26] J.P. Barbier, R.P. Hugel, C. Kappenstein, Copper(III) and nickel(III) diethyldithiocarbamates. An example of copper(II) disproportionation, Inorg. Chim. Acta Lett. 77 (1983) 117–118.
[27] A. Avdeef, J.P. Fackler, R.G. Fischer, Structural characterization of tris(N,N-di-n-butyldithiocarbamato)nickel(IV) bromide. A Ni-S6 complex with unusual chemical properties, J. Am. Chem. Soc. 92 (1970) 6972–6974.
[28] J.P. Fackler, A. Avdeef, R.G. Fischer, Sulfur chelates. XVI. Chemical properties of oxidized nickel(II) dithiocarbamates. X-ray crystal structure of tris(N,N-dibutyldithio-carbamato)nickel(IV)bromide, $NiC_{27}H_{54}N_3S_6Br$, J. Am. Chem. Soc. 95 (1973) 774–782.
[29] C.L. Raston, A.H. White, D. Petridis, D. Taylor, Crystal structure of tris(NN-diethyldithiocarbamato)iron(IV) pentaiodide, J. Chem. Soc. Dalton Trans. (1980) 1928–1931.
[30] V.F. Plyusnin, V.P. Grivin, N.M. Bazhin, E.P. Kuznetzova, S.V. Larionov, Photochemistry of dithiocarbamate complexes of Ni(IV). I. Processes of photoreduction of complexes, J. Photochem. Photobiol. A.: Chem. 74 (1993) 121–127.
[31] V.F. Plyusnin, V.P. Grivin, N.M. Bazhin, E.P. Kuznetzova, S.V. Larionov, Photochemistry of dithiocarbamate complexes of Ni(IV). II. Mechanism of photochromic transformations, J. Photochem. Photobiol. A.: Chem. 74 (1993) 129–135.
[32] G.L. Miessler, E. Zoebisch, L.H. Pignolet, Photochemistry of dithiocarbamato complexes. 2. Photolysis of iron(III) and iron(1V) complexes, Inorg. Chem. 17 (1978) 3636–3644.
[33] K.W. Given, B.M. Mattson, M.F. McGuiggan, G.L. Miessler, L.H. Pignolet, Photochemical reaction pathways of ruthenium(III) complexes. Ultraviolet irradiation of tris(N,N-dialkyldithiocarbamato)ruthenium(III), J. Am. Chem. Soc. 99 (1977) 4855–4857.
[34] M.W. Peterson, R.M. Richman, Photochemical and thermal studies of bis(diethy1dithiocarbamato)dioxomolybdenum, Inorg. Chem. 21 (1982) 2609–2613.
[35] V.F. Plyusnin, V.P. Grivin, S.V. Larionov, Photochemistry of Fe(III), Fe(IV), Ru(III), Mo(VI), and Ni(IV) dithiocarbamate complexes, Coord. Chem. Rev. 159 (1997) 121–133.
[36] B.G. Jeliazkova, N.D. Yordanov, Charge transfer photochemistry of $Cu(Et_2dtc)_2$ and $Cu(dtp)_2$ complexes, Inorg. Chim. Acta 203 (1993) 201–204.
[37] B.G. Jeliazkova, G.C. Sarova, Effect of alcohols on the photochemical reaction of $Cu(Et_2dtc)_2$ in $CHCl_3$, J. Photochem. Photobiol. A: Chem. 97 (1996) 5–9.
[38] V.P. Grivin, V.F. Plyusnin, I.V. Khmelinski, N.M. Bazhin, M. Mitewa, P.R. Bontchev, Pulsed laser photolysis of the $PtCl_6^{2-}$ – creatinine system in methanol, J. Photochem. Photobiol. A.: Chem. 51 (1990) 371–377.
[39] H. Lemmetyinen, R. Ovaskanien, K. Nieminen, K. Vaskonen, I. Sychtchikova, Photolysis of pyrene and chloropyrene in the presence of triethylamine in acetonitrile: dehalogenation assisted by potassium cyanide, J. Chem. Soc. Perkin Trans. 2 (1992) 113–119.
[40] N.V. Tkachenko, L. Rantala, A.Y. Tauber, J. Helaja, P.H. Hynninen, H. Lemmetyinen, Photoinduced electron transfer in phytochlorin-[60]fullerene dyads, J. Am. Chem. Soc. 121 (1999) 9378–9387.
[41] A.R. Hendrickson, R.L. Martin, N.M. Rohde, Dithiocarbamates of nickel in the formal oxidation states I–IV. Electrochemical study, Inorg Chem. 14 (1975) 2980–2985.
[42] J. Lokaj, V. Vrabel, E. Kello, Structure of bis(di-n-butyldithiocarbamato)nickel(II), Chem. Zvesti 38 (1984) 313–320.
[43] D.V. Sokol'skii, I.B. Bersuker, The electronic structure of diethyl dithiocarbamate and its complex with Ni(II); redistribution of charges on coordination and electronic spectra, Teor. Exper. Khim. 8 (1974) 306–310.
[44] F.M. Tulyupa, Y.I. Usatenko, V.S. Barkalov, Electronic spectra of dithiocarbamates, Zhurnal Prikladn. Spektroskop. 9 (1968) 27–32.
[45] Y.V. Ivanov, V.F. Plyusnin, V.P. Grivin, S.V. Larionov, Photochromic transformations of thiuramdisulfide and dithiocarbamate Ni(II) complex in acetonitryl, J. Photochem. Photobiol. A.: Chem. 119 (1998) 33–38.
[46] F. Basolo, R.G. Pearson, Mechanism of Inorganic Reactions. A Study of Metal Complexes in Solution, John Wiley & Sons, New York, 1967, 78 pp.
[47] E. Lindsay, A.Y.S. Malkhasian, C.H. Langford, Solvent dependence of the fast photooxidation of transition-metal maleonitriledithiolate complexes, $[M(S_2C_2(CN)_2)_2]^{2-}$ (M = Ni, Pt), in acetonitrile–chloroform mixtures, Inorg. Chem. 33 (1994) 944–949.
[48] V.F. Plyusnin, E.P. Kuznetzova, G.A. Bogdanchikov, V.P. Grivin, V.N. Kirichenko, S.V. Larionov, Dithiocarbamate radicals in laser flash photolysis of thiuram disulfide and dithiocarbamate anion. Calculation of optical spectra, J. Photochem. Photobiol. A.: Chem. 68 (1992) 299–308.
[49] N.V. Klassen, C.K. Ross, Pulse radiolysis of alkane/carbon tetrachloride glasses and liquids, J. Phys. Chem. 91 (1987) 3668–3672.
[50] A. Hermann, R.M. Wing, Synthesis, stereochemistry, and mechanism of formation of mixed bis(dithio1ato)nickel dimers, Inorg. Chem. 11 (1972) 1415–1420.
[51] H.J. Kruger, R.H. Holm, Chemical and electrochemical reactivity of nickel(II,I) thiolate complexes: examples of ligand-based oxidation and metal-centered oxidative addition, Inorg. Chem. 28 (1989) 1148–1155.
[52] K. Redin, A.D. Wilson, R. Newell, M. Rakowski DuBois, D.L. DuBois, Studies of structural effects on the half-wave potentials of mononuclear and dinuclear nickel(II) diphosphine/dithiolate complexes, Inorg. Chem. 46 (2007) 1268–1276.
[53] D. Huang, L. Deng, J. Sun, R.H. Holm, Cleavage of Ni–(μ2-S)–Ni bridges in dinuclear nickel(II) dithiolate pincer complexes and related reactions, Inorg. Chem. 48 (2009) 6159–6166.
[54] S. Alvarez, R. Vicente, R. Hoffmann, Dimerization and stacking in transition-metal bisdithiolenes and tetrathiolates, J. Am. Chem. Soc. 107 (1985) 6253–6277.
[55] R.H. Furneaux, E. Sinn, Antiferromagnetic copper(II) halide adducts of copper(II) dithiocarbamates, Inorg. Chem. 16 (1977) 1809–1812.
[56] W. Tremel, M. Kriege, B. Krebs, G. Henkel, Nickel-thiolate chemistry based on chelating ligands: controlling the course of self-assembly reactions via ligand bite distances. synthesis, structures, and properties of the homoleptic complexes $[Ni_3(SCH_2C_6H_4CH_2S)_4]^{2-}$ $[Ni_3(SCH_2CH_2S)_4]^{2-}$, and $[Ni_6(SCH_2CH_2CH_2S)_7]^{2-}$, Inorg. Chem. 27 (1988) 3886–3895.